Received: April 6, 2022. Revised: May 6, 2022.

INASS

International Journal of
Intelligent Engineering & Systems

http://www.inass.org/

Aquila Optimizer Based Optimal Allocation of Soft Open Points for Multi-Objective Operation in Electric Vehicles Integrated Active Distribution Networks

Nagaraja Kumari CH[1]* Sai Ram Inkollu[2] Rajesh Patil[3] Varaprasad Janamala[4]

[1]*Guru Nanak Institute of Technology, Ibrahimpatnam, Telangana 501506, India*
[2]*Dhanekula Institute of Engineering & Technology, Vijayawada, Andhra Pradesh 521139, India*
[3]*SVERIS College of Engineering, Pamdharpur, Solarpur, Maharashtra, 413304, India*
[4]*Christ (Deemed to be University), Bangalore, Karnataka 560074, India*
* Corresponding author's Email: nrkumari84@gmail.com

Abstract: The appropriate position and sizing of soft open points (SOPs) for reducing the detrimental impact of electric vehicle (EV) load penetration and renewable energy (RE) variation on active distribution networks (ADNs) are provided in this study. Soft open points (SOPs) have been used to create a multi-objective framework that considers loss minimization and voltage profile enhancement. The non-linear multi-variable complicated SOP allocation problem is solved for the first time using a modern meta-heuristic Aquila optimizer (AO). The modified IEEE 33-bus benchmark and IEEE 69-bus ADNs are used in the simulations. Before SOPs, the average real power loss in IEEE 33-bus AND was 370.329 kW, but after SOPs, it was reduced to 259.356 kW (i.e., 29.96 percent reduction). Similarly, effective SOPs integration in the IEEE 69-bus resulted in a loss reduction of 81.07 percent. AO's computational efficiency is also compared to that of multiobjective particle swarm optimization (MOPSO), particle swarm optimization (PSO), and cuckoo search algorithm (CSA). The AO has produced better results in terms of lower losses, improved voltage profile despite variations in EV load penetration, and RE and load volatility in ADNs, according to the results.

Keywords: Active distribution networks, Aquila optimizer, Electric vehicles, Loss reduction, Renewable energy, Soft open points, Voltage profile improvement.

1. Introduction

The present electric distribution systems (EDSs) are experiencing high penetration levels of renewable energy (RE)-based distributed generation (DG) around the world. Despite their environmental benefits, their intermittency nature has opened up various operational and control issues. In the literature, integration of energy storage systems (ESSs) and optimal network reconfiguration (ONR) are some of the best solutions suggested for overcoming these issues. However, equipping remote control switches (RCSs) in each branch/tie-lines for achieving ONR is a typical and non-economic option. In this scenario, soft open points (SOPs) become popular, which are basically power electronics-based devices that are integrated into EDSs to control active and reactive power flows, regulate voltage, and improve performance under normal operating conditions. Due to their quick response, they are also employed for isolating faulty sections and thereby achieving service restoration and optimal reconfiguration.

In [1], optimal integration of multiple SOPs along with optimal network reconfiguration (ONR) is solved for loss minimization, load balancing under different loading conditions, and distributed generation (DGs) penetration. In [2], ant colony optimization (ACO) and the taxi-cab algorithm (TCA) are employed for NR and SOPs allocation, respectively. The objective function is formulated for loss minimization, load balancing, and DG penetration maximization under variable DG penetration. In [3], the annual cost of losses is

minimized by optimizing the integration of SOPs using a mixed-integer second-order cone model (MISOCM). Multi-objective particle swarm optimization (MOPSO) and TCA are used in [4] to solve optimal network reconfiguration problems as well as optimal SOP allocation by aiming for loss reduction, load balancing, and voltage profile improvement while taking into account different DG penetration levels. In [5], the impact of unbalanced conditions due to asymmetric DG integration is neutralized by solving optimal SOP allocation towards minimizing losses and voltage and current unbalances using semidefinite programming (SDP). In [6], a hybrid approach using ACO and TCA is employed for optimal reconfiguration and SOP allocation by aiming for maximum DG penetration. MISOCM is used in [7] to solve optimal sizing of distributed energy storage systems (DESSs) in active distribution networks (ADNs) by taking into account optimal controls of SOPs-based reconfiguration, tap-changer, and time-of-use (TOU) demand response. The goal of [8] is to optimize performance by utilizing reactive power support of optimal SOP controls and direct load control (DLC) of thermostatically controlled air-conditioning loads. In [9], SOCP-based column-and-constraint generation (C&CG) algorithm is developed for improving EDS performance with optimal SOP controls under photovoltaic (PV) system uncertainty. In [10], a discrete-continuous hyper-spherical search algorithm (DC-HSS) is proposed for solving simultaneous allocation of SOPs and DGs along with optimal NR by focusing on the minimization of distribution SOP losses at different loading conditions. In the presence of uncertainty in network net-loading due to DG power and electric vehicle (EV) charging, the optimal controls of SOPs are proposed for regulating the voltage profile and network congestion in ADNs [11]. In [12], a two-stage robust optimization (RO) via SOCP-based C&CG algorithm is utilized for controlling the SOPs optimally under P and PQ control modes with respect to uncertainty in PV and wind turbine (WT) systems. In [13], building thermal storage (BTS) is suggested for increasing the penetration of renewable energy systems (RESs) using optimal controls of SOPs by a hybrid stochastic/RO approach. In [14], SOPs-based ONR is proposed for handling DGs' uncertainty and thus to maximize the hosting capacity (HC) of practical EDS using a modified version of the MOPSO. In [15], PSO is used to control multiple SOPs optimally, so optimal allocation of DGs and ONR is achieved for loss minimization. In [16], simultaneous ONR and SOPs allocation is proposed for enhancing DG penetration and voltage stability indices and also loss minimization under different load growth scenarios using the Archimedes optimization algorithm (AOA). In [17], the CPLEX optimizer in general algebraic modelling system (GAMS) software is used for conservation voltage reduction (CVR) for peak load reduction and, consequently, energy loss reduction by extracting optimal volt/VAr controls using SOPs in ADNs. In [18], genetic algorithm (GA) is proposed for effective control of active and reactive power flows and thus to optimize performance in RES integrated with SOPs.

In view of the aforementioned research, it is clear that SOPs are basically used to regulate the power flows in the ADNs integrated with RE and/or ESSs. However, the literature works on optimal allocation of SOPs is not much focused on their effectiveness considering emerging EV load and their negative impact on ADNs' performance. Also, the coordinative operation between SOPs and WTs for regulating voltage profile of the ADNs is not emphasized. Thus, our main research is to control SOPs and WTs optimally for maximizing ADNs performance under variable RE, EVs and network loads. In addition, meta-heuristic algorithms are highly adapted in electrical engineering optimization problems. According to no-free-launch (NFL) theorem [19], there is no such single algorithm which can solve all kinds of optimization problems. Thus, researchers are inspired to introduce various new optimization algorithms and/or improvements in the existing algorithms. In recent times, darts game optimizer (DGO) [20], three influential members based optimizer (TIMBO) [21], random selected leader based optimizer (RSLBO) [22], football game based optimization (FGBO) [23], puzzle optimization algorithm (POA) [24], ring toss game-based optimization (RTGBO) [25] are some of such meta-heuristic algorithms. In this aspect, we have introduced a simple and efficient Aquila optimizer (AO) [26], inspired by foraging behaviour and unique hunting skills of Aquila' bird, for solving the proposed multi-objective function and compared its effectiveness with other algorithms. The following are the key contributions of this paper.

- Optimal location and sizing of SOPs are proposed for mitigating the negative impact of EV load penetration on EDNs.
- A multi-objective framework considering loss minimization and voltage profile improvement has been developed using SOPs.
- For the first time, a recent meta-heuristic AO is proposed to solve the non-linear multi-variable complex SOP allocation problem.

- Simulations are performed on the modified IEEE 33-bus benchmark [27] and for different scenarios.

The rest of the paper is organised as follows: Section 2 models SOPs and EV load penetration. Also, modelling of RE variation and network load variability are covered. A multi-objective optimization with real power losses and voltage deviation index is described in Section 3. The concept of AO and its mathematical modelling are given in Section 4. Section 5 presents simulation findings for various EV load penetration situations using a modified IEEE 33-bus benchmark test system and IEEE 69-bus ADN. Section 6 summarised the article's major contributions and research findings.

2. Modelling of SOPs and EV load

In this section, the mathematical modelling of SOPs and EV load penetration, hourly variation in RE and network load profile are explained.

2.1 Power injection modelling of SOPs

In this work, SOPs are considered as VSCs with back-to-back connections that are preferably integrated at normally-open points in EDSs. Considering bus-*i* and bus-*j* as open-points on feeders 1 and 2, respectively, single SOP connection is shown in Fig. 1.

The converter associated to one feeder is converted AC/DC and then transmitted via DC link, and then injected into the other feeder via DC/AC converter. The active power transfer in DC link is the power injection at both the VSCs. For lossless operation,

$$P_{VSC,i} = -P_{VSC,j} \tag{1}$$

The following are the associated constraints considered for SOPs:

$$\sqrt{P_{VSC,i}^2 + Q_{VSC,i}^2} \leq S_{VSC,i} \tag{2}$$

$$\sqrt{P_{VSC,j}^2 + Q_{VSC,j}^2} \leq S_{VSC,j} \tag{3}$$

$$V^{min} \leq \left|V_{VSC,i}\right| \leq V^{max} \tag{4}$$

$$V^{min} \leq \left|V_{VSC,j}\right| \leq V^{max} \tag{5}$$

where $P_{VSC,i}$ and $P_{VSC,j}$ are the active power injections of both VSCs, respectively; $Q_{VSC,i}$ and

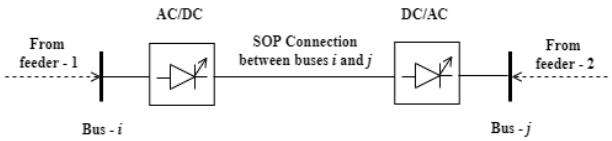

Figure. 1 B2B VSC topology for SOPs in EDN

$Q_{VSC,j}$ are the reactive power injections of both VSCs, respectively; $S_{VSC,i}$ and $S_{VSC,j}$ are the MVA rating of both VSCs, respectively; $\left|V_{VSC,i}\right|$ and $\left|V_{VSC,j}\right|$ are the AC voltage magnitudes of both converters, respectively; V^{min} and V^{max} are the minimum and maximum voltage magnitude limits, respectively.

2.2 Hourly EV load penetration

The EV load penetration is expressed in terms of percentage to the base load, as expressed by,

$$P_{ev,i(h)} = \rho_{ev(h)} \times P_{d,i(0)} \times \left(\frac{|V_i|}{|V_r|}\right)^{\alpha_{ev}} \tag{6}$$

$$Q_{ev,i(h)} = P_{ev,i(h)} \times tan(\emptyset_{ev}) \times \left(\frac{|V_i|}{|V_r|}\right)^{\beta_{ev}} \tag{7}$$

where $P_{ev,i(h)}$ and $Q_{ev,i(h)}$ are the hourly real and reactive penetration levels of EV load, respectively; $\rho_{ev(h)}$ is the EV load penetration level, $P_{d,i(0)}$ and $Q_{d,i(0)}$ are the initial real and reactive powers loads of bus-*i*, respectively; α_{ev} and β_{ev} are the power exponential coefficients as per voltage dependent load modelling [28], $\emptyset_{ev}$ is the operating power factor of EV charging converter, $|V_i|$ and $|V_r|$ are the voltage magnitude of bus-*i* and reference bus, respectively.

2.3 Hourly variability in PV and WT generation

The variability in solar PV system and WT generation is expressed in terms of percentage to their maximum installed capacity, as given by,

$$P_{pv,i(h)} = \rho_{pv(h)} \times P_{PV,i(c)} \tag{8}$$

$$P_{wt,i(h)} = \rho_{wt(h)} \times P_{WT,i(c)} \tag{9}$$

$$Q_{wt,i(h)} = P_{wt,i(h)} \times tan\left(\emptyset_{wt(h)}\right) \tag{10}$$

where $P_{pv,i(h)}$ and $P_{wt,i(h)}$ are the hourly real power generations by PV and WT systems, respectively; $P_{PV,i(c)}$ and $P_{WT,i(c)}$ are the installed capacity of PV and WT systems, respectively; $\rho_{pv(h)}$ and $\rho_{wt(h)}$ are the variability factors of PV and WT generations, respectively; $Q_{wt,i(h)}$ is the hourly reactive power

generation by WT systems, $\emptyset_{wt}$ is the operating power factor angle of the WT system during hour-*h*.

2.4 Hourly variability in net loading profile

Finally, by considering EV load penetration, PV and WT generations, the hourly net loading profile of the AND is modelled as, the variability in solar PV system and WT generation is expressed in terms of percentage to their maximum installed capacity, as given by,

$$P_{d,i(h)} = \gamma_{l(h)} P_{d,i(0)} + P_{ev,i(h)} - P_{pv,i(h)} - P_{wt,i(h)} \quad (11)$$

$$Q_{d,i(h)} = \gamma_{l(h)} Q_{d,i(0)} + Q_{ev,i(h)} - Q_{wt,i(h)} \quad (12)$$

where $P_{d,i(0)}$ and $Q_{d,i(0)}$ are the initial real and reactive powers loads of bus-*i*, respectively; $P_{d,i(h)}$ and $Q_{d,i(h)}$ are the net real and reactive power loads including EV load, PV and WT generations at bus-*i*, respectively; $\gamma_{l(h)}$ is the scaling factor to define hourly variation in network load profile.

3. Problem formulation

Minimization of distribution losses and voltage profile improvement are considered to formulate multi-objective function, as defined, by,

$$OF = min\{P_{loss} + VDI\} \quad (13)$$

$$P_{loss} = \sum_{k=1}^{nbr} I_k^2 r_k \quad (14)$$

$$VDI = \frac{1}{nbus} \sum_{i=1}^{nbus} \left|1 - |V_i|\right| \quad (15)$$

where P_{loss} is the total real distribution losses, VDI is the voltage deviation index, nbr and $nbus$ are the number of branches and buses in the network, respectively; I_k and r_k are the current flow and resistance of branch-*k*, respectively.

In addition to the constraints given in Eqs. (2) to (5), the following are the other major operational and planning constraints associated to the proposed multi-objective function:

$$V^{min} \le |V_i| \le V^{max}, i \forall nbus \quad (16)$$

$$I_k \le {I_k}^{max}, k \forall nbr \quad (17)$$

$$0.3 \le \emptyset_{wt} \le 1.0, i \forall nwt \quad (18)$$

where $\emptyset_{wt}$ is operating power factor angle of the WTs to extract reactive power support as per the network operational requirements, nwt is the number of WTs in the network.

4. Aquila optimizer

In 2021, Aquila optimizer (AO) is introduced as a new nature-inspired meta-heuristic optimization algorithm. The behaviour of the Aquila, which is one of the most prevalent birds of prey in the Northern Hemisphere and belongs to the Accipitridae family, was the inspiration for AO. Its computational efficiency over various algorithms is well described and proved as superior [26]. This section delves into the mathematical modelling of Aquila's bird hunting skills.

In similar to all population algorithms, AO begins with the random generation of population for candidate solution (X) using their lower and upper bounds as given by,

$$X_{ij} = l_j + rand \times (u_j - l_j) \quad (19)$$

where $i = 1{:}\, n_p$ and $j = 1{:}\, d_s$; n_p and d_s are denote the total population/ candidate solutions and number of dimensions, respectively; u_j and l_j are the upper and lower bounds of *j*th candidate, respectively; $rand$ is a random number.

The best candidate solution for this initial random population will be evaluated in the initial phase and carried forward to the iterative phase to determine the global best candidate solution.

Aquila seeks the best hunting area in the first iteration phase after recognizing the prey by maintaining a high soar with vertical stoop. This is known as expanded exploration and its mathematical expression is given by,

$$X_1(k+1) = X_{best}(k) \times \left(1 - \frac{k}{k_{max}}\right) + [X_m(k) - X_{best}(k) \times rand] \quad (20)$$

where $X_{best}(k)$ is the best candidate solution evaluated in initial phase, $X_1(k+1)$ is the updated solution in first iteration, k and k_{max} are the present and maximum number of iterations, respectively; $(1 - k/k_{max})$ is used to control the expanded exploration, $rand$ is a random number between 0 and 1, $X_m(k)$ is the mean value of all locations of Aquila's movements at iteration *k*, and is given by,

$$X_m(k) = \frac{1}{n_p} \sum_{i=1}^{n} X_i(k); i = 1{:}\, d_s \quad (21)$$

Aquila attempts to reduce its search area in a circle above the pray in the next step of the hunting

process, and prepares to assault the pray. In AO, this phase is known as narrowed exploration, and its mathematical equivalent is proposed by levy flight distribution function, as follows:

$$X_2(k+1) = X_{best}(k) \times Levy(d_s) + X_R(k) + (y - x) \quad (22)$$

$$Levy(d_s) = s \times \frac{u \times \sigma}{|v|^{\frac{1}{\beta}}} \quad (23)$$

$$\sigma = \frac{\Gamma(1+\beta) \times \sin\left(\frac{\pi\beta}{2}\right)}{\Gamma\left(\frac{1+\beta}{2}\right) \times \beta \times 2^{\left(\frac{\beta-1}{2}\right)}} \quad (24)$$

where $X_2(k+1)$ is the updated solution of the next iteration k which is generated by narrowed exploration, $X_R(k)$ is the random solution taken in iteration k , $Levy(d_s)$ is the levy flight distribution function, u and v are random numbers between 1 and 0; s and β are the fixed constants equal to 0.01 and 1.5, respectively; x and y are used to model spiral shape movements by Aquila and given by,

$$y = (a + b \times c) \times \cos\left(-d \times c + \frac{3\pi}{2}\right) \quad (25)$$

$$x = (a + b \times c) \times \sin\left(-d \times c + \frac{3\pi}{2}\right) \quad (26)$$

where a takes a value between 1 and 20 for fixed the number of cycles, $b$is a small fixed value to 0.00565, c is a integer numbers from 1 to d_s, d is a small value fixed to 0.005.

The third phase of AO is called expanded exploitation in which Aquila drops vertically with a preparatory attack to detect the prey reaction once the target region has been correctly specified and the Aquila is ready to land and fight. At this point, Aquila uses the target's chosen location to come near to the prey and attack, a technique known as low flight with slow descending attack and is given by,

$$X_3(k+1) = [X_{best}(k) - X_m(k)] \times \alpha - rand + [(ub - lb) \times rand + lb] \times \delta \quad (27)$$

where $X_3(k+1)$ is the solution of the next iteration of k, which is generated by the low flight with descent attack, $X_{best}(k)$ is the approximate location of the prey until kth iteration, $rand$ is a number between 0 and 1, α and δ are exploitation adjustment parameters and fixed to a small value 0.1.

Narrowed exploitation is the fourth phase of AO, and it is used to mimic the stochastic movement of Aquila's when it is close to and attacking the prey on land. It is also the last stage of Aquilas to seize the pray, and it is given by,

$$X_4(k+1) = Q_f \times X_{best}(k) - [e \times X(k) \times rand] - f \times Levy(d_s) + rand + e \quad (28)$$

$$Q_f = k^{\frac{2 \times rand - 1}{(1 - k_{max})^2}} \quad (29)$$

$$e = 2 \times rand - 1, f = 2 \times \left(1 - \frac{k}{k_{max}}\right) \quad (30)$$

where $Q_f$is a quality function used to balance the search strategies, e denotes various motions of the AO used to track the prey during the elope, and f presents decreasing values from 2 to 0, which denote the flight slope of the AO used to follow the prey during the elope from the first location $X_1(k+1)$ to the last location $X_4(k+1)$ in iteration k.

In comprehension, AO employs the well-known four primary hunting strategies of Aquila, each of which has numerous significant differences, as well as the Aquila's ability to intelligently and quickly switch between hunting methods depending on the situation. Aquila is one of the most smart and skilled hunters, probably second only to humans.

5. Simulation results

Simulations are performed on modified IEEE 33-bus ADN considering different EV load penetration at different timings. The test system has 33 buses interconnected with 32 branches and 3 tie-lines. It has 4 DGs of 200 kW at buses 18, 22, 25 and 33. Also, reactive power compensation devices of 400 kVAr and 600 kVAr are integrated at buses 18 and 33, respectively. The peak load is 3715 kW and 2300 kVAr, respectively. The details bus data, branch data and schematic diagram are given in [20]. In this work, the DGs at bus-18 and 22 are considered as solar photovoltaic (PV) sources, and the DGs at 25 and 33 are considered as wind turbine (WT) sources with variable power factor control between 0.3 and 1. Thus, the required reactive power compensation is aimed to extract from WTs itself by neglecting CBs at buses 18 and 33. Under these modifications, identification of best locations for SOPs connection and optimal control of WTs' power factors are treated as search space while solving the proposed multi-objective function. The hourly load profile, generations of PV and WTs are determined based on data in [29].

Table 1. Forecasted values of network load and EV load profiles, PV and WT generations (%)

Hr	$\rho_{ev(h)}$	$\rho_{wt(h)}$	$\rho_{pv(h)}$	$\rho_{l(h)}$
1	0.719	0.815	0	0.783
2	0.674	0.88	0	0.738
3	0.624	0.886	0	0.723
4	0.588	0.88	0	0.708
5	0.582	0.881	0	0.699
6	0.588	0.881	0	0.678
7	0.6	0.953	0	0.663
8	0.633	0.987	0.008	0.708
9	0.644	0.985	0.050	0.801
10	0.73	0.962	0.125	0.801
11	0.793	1	0.418	0.843
12	0.844	0.979	0.511	0.873
13	0.875	0.945	0.516	0.889
14	0.868	0.776	0.475	0.916
15	0.851	0.673	0.418	0.889
16	0.875	0.591	0.254	0.889
17	0.951	0.487	0.050	0.879
18	1	0.466	0	0.843
19	0.981	0.373	0	0.864
20	0.948	0.339	0	0.976
21	0.9	0.339	0	1
22	0.875	0.372	0	0.976
23	0.801	0.393	0	0.964
24	0.722	0.339	0	0.889

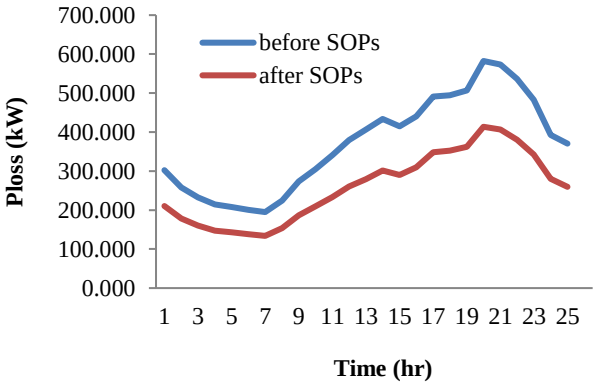

Figure. 2 Comparison of P_{loss} before and after SOPs

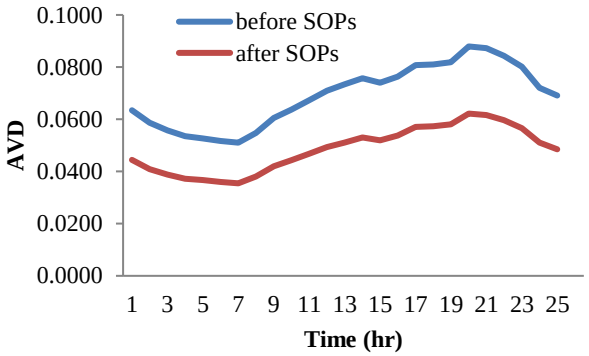

Figure. 3 Comparison of AVD before and after SOPs

The simulations are performed for each hour considering respective variability in EV load penetration, network load variability, and PV and WT generations as given in Table 1. For instant, at hour-13, the EV load penetration is around 87.5% to the network base load of 3715 kW ($\rho_{ev(13)}$ = 0.875), WT generation is 94.5% of 200 kW capacity ($\rho_{wt(13)}$= 0.945), PV generation is 51.6% of 200 kW capacity ($\rho_{pv(13)}$ =0.516) and variation in network load is 88.9% of 3715 kW ($\rho_{pv(13)}$=0.889), respectively.

By modifying the loads at each bus as per these variations, Newton Raphson (NR) load flow [30] is performed for each hour. The network performance without SOPs is given in Table 2. At this stage, the WTs power factor is not controlled optimally and it is fixed to $\cos\emptyset_{wt}$=1, thus, reactive power support from WTs is zero. As a result, the net effective real and reactive powers loading on the network are become as 5573.37 kW and 2943.47 kVAr, respectively. Correspondingly, the incurred losses are 406.479 kW and 268.993 kVAr, respectively. Also, the minimum voltage magnitude is observed as 0.8762 p.u. at bus-18. On the other hand, the average voltage deviation is noted as 0.0734 p.u. A similar conclusion can be drawn for each hour the same Table 2.

By using the proposed AO, the optimal location and sizes of SOP connection in the network is determined towards multi-objective function defined in Eq. (13). The best open-points on the network for SOPs integration are bus-12 and 22, respectively. Since, the net effective loading is changing in each hour, the MVA rating of SOPs are determined for each hour, as given in Table 3. From all the hours, the minimum and maximum ratings of VSC at bus-12 are 0.825 and 1.356 MVA, and at bus-22, they are 0.83 MVA and 1.372 MVA, respectively.

Now, by having optimized SOPs and WTs' power factor controls, the improved performance of the network is also given in Table 2, for each hour. In comparison, the real and reactive power losses are decreased, voltage profile is increased significantly. For instant, at hour 13, the incurred losses now are 279.695 kW and 215.557 kVAr, respectively. Also, the minimum voltage magnitude is observed as 0.9099 p.u. at bus-32. On the other hand, the average voltage deviation is noted as 0.0511p.u. A similar conclusion can be drawn for each hour the same Table 2.

A comparative understanding of the optimal SOPs and WTs' power factor controls in the network are given in Fig. 2 and Fig. 3, for real power losses and AVD, respectively. From these, it can be said that the proposed AO approach for

Table 2. Hourly network performance without and with SOPs and WT power factor controls

Hr	P_d (kW)	Q_d (kVAr)	Without SOPs and WTs pf control				With SOPs and WTs pf control			
			P_{loss} (kW)	Q_{loss} (kVAr)	$V_{min(18)}$ (p.u)	VDI	P_{loss} (kW)	Q_{loss} (kVAr)	$V_{min(32)}$ (p.u)	VDI
1	4928.95	2431.06	301.989	200.856	0.8897	0.0635	210.097	163.385	0.9236	0.0444
2	4588.94	2252.81	257.761	171.459	0.8978	0.0587	178.441	139.016	0.9302	0.0409
3	4367.67	2154.27	232.717	154.823	0.9029	0.0557	160.644	125.230	0.9339	0.0389
4	4196.87	2074.40	214.135	142.474	0.9068	0.0535	147.610	115.111	0.9367	0.0373
5	4143.46	2044.01	208.093	138.455	0.9081	0.0527	143.413	111.862	0.9377	0.0367
6	4085.02	1994.52	200.490	133.385	0.9098	0.0517	138.329	107.931	0.9390	0.0360
7	4039.65	1967.28	194.987	129.745	0.9107	0.0510	133.879	104.629	0.9404	0.0355
8	4297.71	2124.11	224.350	149.274	0.9043	0.0548	153.742	120.073	0.9359	0.0380
9	4663.10	2387.46	273.661	182.014	0.8948	0.0605	187.016	145.690	0.9283	0.0420
10	4922.92	2494.60	304.429	202.220	0.8898	0.0637	209.246	162.620	0.9238	0.0444
11	5152.12	2695.37	340.597	225.539	0.8859	0.0672	233.272	180.250	0.9184	0.0467
12	5401.18	2852.19	379.325	251.005	0.8804	0.0709	260.306	200.716	0.9133	0.0493
13	5573.37	2943.47	406.479	268.993	0.8762	0.0734	279.695	215.557	0.9099	0.0511
14	5734.84	3009.52	433.579	287.067	0.8724	0.0757	301.245	231.865	0.9057	0.0530
15	5643.06	2907.65	414.693	274.634	0.8752	0.0740	290.420	223.492	0.9073	0.0520
16	5819.77	2943.47	440.120	291.930	0.8701	0.0763	310.022	239.057	0.9044	0.0537
17	6153.81	3032.20	491.241	326.471	0.8611	0.0807	348.679	269.539	0.8991	0.0571
18	6208.36	3006.05	494.878	328.985	0.8602	0.0810	352.691	272.848	0.8990	0.0574
19	6261.58	3036.59	506.618	336.820	0.8589	0.0819	362.352	280.036	0.8969	0.0581
20	6583.58	3307.30	582.418	387.442	0.8487	0.0879	413.708	319.526	0.8888	0.0622
21	6516.11	3298.41	573.418	381.511	0.8499	0.0873	406.624	314.020	0.8895	0.0617
22	6332.18	3190.55	535.959	356.554	0.8549	0.0844	380.068	293.612	0.8934	0.0596
23	6037.73	3044.62	483.298	321.524	0.8622	0.0801	342.538	264.664	0.8989	0.0566
24	5522.93	2725.90	392.652	261.147	0.8762	0.0721	280.506	216.643	0.9086	0.0511

Table 3. Hourly optimized SOPs ratings at buses 12 and 22 with WT power factor controls

Hr	SOP_{12} (MVA)	SOP_{22} (MVA)	Hr	SOP_{12} (MVA)	SOP_{22} (MVA)
1	1.009	1.017	13	1.166	1.178
2	0.938	0.945	14	1.197	1.210
3	0.893	0.900	15	1.172	1.184
4	0.859	0.865	16	1.202	1.215
5	0.847	0.853	17	1.261	1.275
6	0.834	0.840	18	1.267	1.281
7	0.825	0.830	19	1.278	1.293
8	0.880	0.887	20	1.356	1.372
9	0.963	0.971	21	1.344	1.360
10	1.015	1.024	22	1.304	1.319
11	1.075	1.085	23	1.243	1.256
12	1.130	1.141	24	1.130	1.141

SOPs integration has improved the network performance irrespective of EVs penetration levels and RE and load variations.

The computational efficiency of AO is compared with MOPSO [4], in which network load profile and DGs power variation are only considered while solving SOPs allocation problem in IEEE 69-bus test system. In addition to AO, the problem is solved with PSO [31], cuckoo search algorithm (CSA) [32], differential squirrel search algorithm (DSSA) [33]. The comparative results are given in Table 4.

From the results, it is observed that the optimal SOPs at bus-2 and bus-61 are resulted for 81.07% loss reduction in comparison to base case. Though AO outperforms MOPSO, PSO, and CSA, DSSA is also a competitive algorithm in terms of global optima. However, based on the NFL [19], it is

Table 4. Comparison of AO performance with MOPSO [4], PSO [31], CSA [32] and DSSA [33]

Algorithm	bus-*i*	bus-*j*	P_{inj_i} (MW)	Q_{inj_i} (MVAr)	S_{inj_i} (MVA)	P_{inj_j} (MW)	Q_{inj_j} (MVAr)	S_{inj_j} (MVA)	P_{loss} (kW)	Loss Reduction
Base	-	-	-	-	-	-	-	-	225	-
MOPSO	50	59	-	-	5.00	-	-	5.00	60.00	73.33 %
PSO	59	47	2.61	0.87	2.75	-2.61	0.36	2.63	63.39	71.83 %
CSA	62	48	2.14	0.50	2.20	-2.14	2.57	3.34	57.16	74.60 %
DSSA	61	2	1.37	0.71	1.55	-1.37	2.48	2.84	42.60	81.06 %
AO	61	2	1.38	0.71	1.55	-1.38	2.48	2.84	42.59	81.07 %

necessary to compare the computational efficiency of the AO to that of other recent algorithms. This has been considered as a future extension and scope of this work.

6. Conclusion

Integration of renewable energy (RE) sources and adoption of electric vehicles (EVs) has become a popular strategy for combating global warming and ensuring a sustainable energy supply. Their intermittency and stochastic nature, on the other hand, posed a number of issues in electrical distribution networks (EDNs). The influence of variability in active distribution networks (ADNs) due to photovoltaic (PV), wind turbine (WT), and electric vehicle (EV) load on network loads is mitigated in this paper using an Aquila optimizer (AO) based optimal allocation of soft open points (SOPs). IEEE 33-bus and 69-bus ADNs are used in the simulations. When the findings of AO are compared to those of other heuristic approaches, it is clear that the proposed approach for adjusting real-time toward flexible and optimum functioning in ADNs with evolving trends is superior, supporting the proposed approach.

Conflicts of Interest

The authors declare no conflict of interest.

Author Contributions

The supervision, review of work and project administration, has been done by Nagaraja Kumari.CH. The paper background work, conceptualization, and methodology have been done by Sai Ram Inkollu. The dataset collection and editing draft is prepared by Rajesh Patil. The program implementation, result analysis and comparison, and visualization have been done by Varaprasad Janamala.

References

[1] W. Cao, J. Wu, N. Jenkins, C. Wang, and T. Green, "Benefits analysis of soft open points for electrical distribution network operation", *Applied Energy*, Vol. 165, pp. 36-47, 2016.

[2] Q. Qi, J. Wu, L. Zhang, and M. Cheng, "Multi-objective optimization of electrical distribution network operation considering reconfiguration and soft open points", *Energy Procedia*, Vol. 103, pp. 141-146, 2016.

[3] C. Wang, G. Song, P. Li, H. Ji, J. Zhao, and J. Wu, "Optimal configuration of soft open point for active distribution network based on mixed-integer second-order cone programming", *Energy Procedia*, Vol. 103, pp. 70-75, 2016.

[4] Q. Qi, J. Wu, and C. Long, "Multi-objective operation optimization of an electrical distribution network with soft open point, *Applied Energy*, Vol. 208, pp. 734-744, 2017.

[5] P. Li, H. Ji, C. Wang, J. Zhao, G. Song, F. Ding, and J. Wu, "Optimal operation of soft open points in active distribution networks under three-phase unbalanced conditions", *IEEE Transactions on Smart Grid*, Vol. 10, No. 1, pp. 380-391, 2019.

[6] Q. Qi and J. Wu, "Increasing distributed generation penetration using network reconfiguration and soft open points", *Energy Procedia*, Vol. 105, pp. 2169-2174, 2017.

[7] L. Bai, T. Jiang, F. Li, H. Chen, and X. Li, "Distributed energy storage planning in soft open point based active distribution networks incorporating network reconfiguration and DG reactive power capability", *Applied Energy*, Vol. 210, pp. 1082-1091, 2018.

[8] Q. Wang, J. Liao, Y. Su, C. Lei, T. Wang, and N. Zhou, "An optimal reactive power control method for distribution network with soft normally-open points and controlled air-conditioning loads", *International Journal of Electrical Power & Energy Systems*, Vol. 103, pp. 421-430, 2018.

[9] H. Ji, C. Wang, P. Li, F. Ding, and J. Wu, "Robust operation of soft open points in active distribution networks with high penetration of photovoltaic integration", *IEEE Transactions on Sustainable Energy*, Vol. 10, No. 1, pp. 280-289, 2019.

[10] I. Diaaeldin, S. A. Aleem, A. E. Rafei, A. Abdelaziz, and A. F. Zobaa, "Optimal network reconfiguration in active distribution networks with soft open points and distributed generation", *Energies*, Vol. 12, No. 21, 4172, 2019.

[11] H. Hafezi and H. Laaksonen, "Autonomous soft open point control for active distribution network voltage level management", In: *Proc. of 2019 IEEE Milan PowerTech*, pp. 1-6, 2019.

[12] P. Cong, Z. Hu, W. Tang, C. Lou, and L. Zhang, "Optimal allocation of soft open points in active distribution network with high penetration of renewable energy generations", *IET Generation, Transmission & Distribution*, Vol. 14, No. 26, pp. 6732-6740, 2020.

[13] T. Zhang, J. Wang, H. Zhong, G. Li, M. Zhou, and D. Zhao, "Soft open point planning in renewable-dominated distribution grids with

building thermal storage", *CSEE Journal of Power and Energy Systems*, pp. 1-9, 2020.

[14] I. M. Diaaeldin, S. H. A. Aleem, A. E. Rafei, A. Y. Abdelaziz, and A. F. Zobaa, "Enhancement of hosting capacity with soft open points and distribution system reconfiguration: Multi-objective bilevel stochastic optimization", *Energies*, Vol. 13, No. 20, p. 5446, 2020.

[15] E. Karunarathne, J. Pasupuleti, J. Ekanayake, and D. Almeida, "The optimal placement and sizing of distributed generation in an active distribution network with several soft open points", *Energies*, Vol. 14, No. 4, p. 1084, 2021.

[16] Z. M. Ali, I. M. Diaaeldin, A. E. Rafei, H. M. Hasanien, S. H. Aleem, and A. Y. Abdelaziz, "A novel distributed generation planning algorithm via graphically-based network reconfiguration and soft open points placement using Archimedes optimization algorithm", *Ain Shams Engineering Journal*, Vol. 12, No. 2, pp. 1923-1941, 2021.

[17] V. B. Pamshetti, S. Singh, A. K. Thakur, and S. P. Singh, "Multistage coordination volt/VAR control with CVR in active distribution network in presence of inverter-based DG units and soft open points", *IEEE Transactions on Industry Applications*, Vol. 57, No. 3, pp. 2035-2047, 2021.

[18] A. Farzamnia, S. Marjani, S. Galvani, and K. T. Kin, "Optimal Allocation of Soft Open Point Devices in Renewable Energy Integrated Distribution Systems", *IEEE Access*, Vol. 10, pp. 9309-9320, 2022.

[19] S. P. Adam, S. A. Alexandropoulos, P. M. Pardalos, and M. N. Vrahatis, "No free lunch theorem: A review. Approximation and optimization", *Approximation and Optimization, Springer Optimization and Its Applications*, Vol. 145, pp. 57-82, 2019.

[20] M. Dehghani, Z. Montazeri, H. Givi, J. M. Guerrero, and G. Dhiman, "Darts game optimizer: A new optimization technique based on darts game", *Int. J. Intell. Eng. Syst*. Vol. 13, No. 5, pp. 286-294, 2020, doi: 10.22266/ijies2020.1031.26.

[21] F. A. Zeidabadi, M. Dehghani, and O. P. Malik, "TIMBO: Three Influential Members Based Optimizer", *Int. J. Intell. Eng. Syst*. Vol. 14, No. 5, pp. 121-128, 2021, doi: 10.22266/ijies2021.1031.12.

[22] F. A. Zeidabadi, M. Dehghani, and O. P. Malik, "RSLBO: Random Selected Leader Based Optimizer", *Int. J. Intell. Eng. Syst*., Vol. 14, No. 5, pp. 529-38, 2021, doi: 10.22266/ijies2021.1031.46.

[23] M. Dehghani, M. Mardaneh, J. M. Guerrero, O. Malik, and V. Kumar, "Football game based optimization: An application to solve energy commitment problem", *Int. J. Intell. Eng. Syst.*, Vol. 13. No. 5, pp. 514-523, 2020, doi: 10.22266/ijies2020.1031.45.

[24] F. A. Zeidabadi and M. Dehghani, "POA: Puzzle optimization algorithm", *Int. J. Intell. Eng. Syst.* Vol. 15, No. 1, pp. 273-281, 2022, doi: 10.22266/ijies2022.0228.25.

[25] S. A. Doumari, H. Givi, M. Dehghani, and O. P. Malik, "Ring Toss Game-Based Optimization Algorithm for Solving Various Optimization Problems", *Int. J. Intell. Eng. Syst.* Vol. 14, No. 3, pp. 545-554, 2021, doi: 10.22266/ijies2021.0630.46.

[26] L. Abualigah, D. Yousri, M. A. Elaziz, A. A. Ewees, M. A. A. Qaness, and A. H. Gandomi, "Aquila optimizer: a novel meta-heuristic optimization algorithm", *Computers & Industrial Engineering*, Vol. 157, 107250, 2021.

[27] S. H. Dolatabadi, M. Ghorbanian, P. Siano, and N. D. Hatziargyriou, "An enhanced IEEE 33 bus benchmark test system for distribution system studies", *IEEE Transactions on Power Systems*, Vol. 36, No. 3, pp. 2565-2572, 2020.

[28] V. Janamala and D. S. Reddy, "Coyote optimization algorithm for optimal allocation of interline–Photovoltaic battery storage system in islanded electrical distribution network considering EV load penetration", *Journal of Energy Storage*, Vol. 41, 102981, 2021.

[29] R. B. Navesi, D. Nazarpour, R. Ghanizadeh, and P. Alemi, "Switchable Capacitor Bank Coordination and Dynamic Network Reconfiguration for Improving Operation of Distribution Network Integrated with Renewable Energy Resources", *Journal of Modern Power Systems and Clean Energy*, pp. 1-12, 2021

[30] R. D. Zimmerman, C. E. M. Sánchez, and R. J. Thomas, "MATPOWER: Steady-state operations, planning, and analysis tools for power systems research and education", *IEEE Transactions on Power Systems*, Vol. 26, No. 1, pp. 12-19, 2011.

[31] J. Kennedy and R. Eberhart, "Particle swarm optimization", In: *Proc. of ICNN'95-International Conference on Neural Networks*, Vol. 4, pp. 1942-1948, 1995.

[32] A. H. Gandomi, X. S. Yang, and A. H. Alavi, "Cuckoo search algorithm: a metaheuristic approach to solve structural optimization problems", *Engineering with Computers*, Vol. 29, No. 1, pp. 17-35, 2013.

[33] B. Jena, M. K. Naik, A. Wunnava, and R. Panda, "A Differential Squirrel Search Algorithm", *Advances in Intelligent Computing and Communication, Lecture Notes in Networks and Systems*, Vol. 202, pp. 143-152, 2021.